Design and characterization of single-mode holey fibers with low bending losses

Yukihiro Tsuchida, Kunimasa Saitoh, and Masanori Koshiba

Division of Media and Network Technologies, Hokkaido University, Sapporo 060-0814, Japan
yukihiro@icp.ist.hokudai.ac.jp

Abstract: As the fiber-to-the-home network construction increased, optical fiber cables are demanded to be easier to handle and require less space. Under this situation, a single mode fiber (SMF) permitting small bending radius is strongly requested. In this paper, we propose and demonstrate a novel type of bending-insensitive single-mode holey fiber which has a doped core and two layers of holes with different air-hole diameters. The fiber has a mode field diameter of 9.3 μm at 1.55 μm and a cutoff wavelength below 1.1 μm, and shows a bending loss of 0.011 dB/turn at 1.55 μm for bending radius of 5 mm and a low splice loss of 0.08 dB per fusion-splicing to a conventional SMF.

OCIS codes: (060.2330) Fiber optics communications; (060.2280) Fiber design and fabrication.

References and links

1. P.St.J. Russell, "Photonic crystal fibers," Science **299**, 358-362 (2003).
2. T. Hasegawa, E. Sasaoka, M. Onishi, M. Nishimura, Y. Tsuji, and M. Koshiba, "Novel hole-assisted lightguide fiber exhibiting large anomalous dispersion and low loss below 1 dB/km," in proceedings of Optical Fiber Communication Conference (OFC2001), paper PD5, Anaheim, USA, (2001).
3. T. Hasegawa, E. Sasaoka, M. Onishi, M. Nishimura, Y. Tsuji, and M. Koshiba, "Hole-assisted lightguide fiber for large anomalous dispersion and low optical loss," Opt. Express **9**, 681-686 (2001), http://www.opticsexpress.org/abstract.cfm?URI=OPEX-9-13-681.
4. K. Nakajima, K. Hogari, J. Zhou, K. Tajima, and I. Sankawa, "Hole-assisted fiber design for small bending and splice losses," IEEE Photon. Technol. Lett. **15**, (1737-1739) 2003.
5. T. Hasegawa, T. Saitoh, D. Nishioka, E. Sasaoka, and T. Hosoya, "Bending-insensitive single-mode holey fiber with SMF-compatibility for optical wiring applications," in proceedings of European Conference on Optical Communications (ECOC2003), paper We2.7.3, Rimini, Italy, (2003).
6. A. Bjarklev, J. Broeng, and A.S. Bjarklev, *Photonic Crystal Fibres*, Kluwer Academic Publishers, 2003.
7. D. Marcuse, "Loss analysis of single-mode fiber splices," Bell Syst. Tech. J. **56**, 703-718 (1977).
8. D. Marcuse, "Influence of curvature on the losses of doubly clad fibers," Appl. Opt. **21**, 4208-4213 (1982).
9. F.L. Teixeira and W.C. Chew, "General closed-form PML constitutive tensors to match arbitrary bianisotropic and dispersive linear media," IEEE Microwave Guided Wave Lett. **8**, 223-225 (1998).
10. K. Saitoh and M. Koshiba, "Full-vectorial imaginary-distance beam propagation method based on a finite element scheme: application to photonic crystal fibers," IEEE J. Quantum Elencron. **38**, 927-933 (2002).
11. M. Koshiba and K. Saitoh, "Numerical verification of degeneracy in hexagonal photonic crystal fibers," IEEE Photon. Technol. Lett. **13**, 1313-1315 (2001).

1. Introduction

The increasing demand for large capacity and low cost in optical communication systems imposes a great importance on dense and flexible optical wiring, which is realized by optical fibers which operate under small bending radius. However, the standard single-mode fiber (SMF) has a disadvantage that the minimum radius allowed for the fiber to be bent is approximately 30 mm, and therefore a large space has to be occupied when using the SMF. From this point of view, bending-insensitive optical fiber with a small allowed bending radius has been strongly requested.

Recently, photonic crystal fibers [1], also called holey fibers (HFs) or microstructured optical fibers, have been under intensive study. They can offer a number of unique and useful properties not achievable in standard silica glass fibers. Especially, HFs with a Germanium-doped core [2], also known as hole-assisted fibers, have attracted great attention because of their excellent bending loss characteristics. This makes the hole-assisted fibers to be a good candidate for dense and flexible optical wiring in the fiber-to-the-home system. So far, various HFs with low bending loss have been reported [3]-[5]. HFs with low bending loss can be realized by increasing the air-hole diameter, however, the suppression of bending loss usually brings about small mode field diameter (MFD) of the fundamental mode and long cutoff wavelength of the higher-order modes. The former results in optical loss at a splice with a standard SMF, and the latter results in multi-mode operation.

In this paper, we propose and demonstrate a novel type of bending-insensitive single-mode HF which has a raised-index core surrounded by two layers of holes with two different air-hole diameters. We show that it is possible to design a single-mode HF with a MFD matching to a standard SMF and a small allowable bending radius by appropriately choosing the core radius, the hole pitch, and the air-hole diameters. The fabricated HF has a MFD of 9.3 μm at 1.55 μm and a cutoff wavelength below 1.1 μm, and shows a bending loss of 0.011 dB/turn at 1.55 μm for bending radius of 5 mm and a low splice loss of 0.08 dB per fusion-splicing to a conventional SMF.

2. Holey fiber design

For optical wiring application, the fiber should have low bending loss, short cutoff wavelength of the higher-order mode, and a MFD matched with that of the standard SMF. Although these requirements are usually conflicting, they can be realized by HFs. Nakajima *et al.* have investigated the hole-assisted fiber structure with one layer of air-holes in Fig. 1(a) for low bending and splice losses [4]. The HFs with one layer of air-holes have a simple structure, however, they have a problem that suppressing bending loss strengthens also the confinement of higher-order modes and results in long cutoff wavelength of the higher-order modes. In this paper, we consider a HF structure having a Germanium-doped core surrounded by two layers of air holes running along fiber axis, as shown in Fig. 1(b), where a is the radius of the core, d_1 and d_2 are the diameters in the inner and the outer layers, respectively, and Λ is the hole pitch. We should notice that the hole diameters d_1 and d_2 are not necessarily equal, while the hole pitch Λ is uniform in the cross section. This HF structure can be fabricated by using stack-and-draw fabrication process [6].

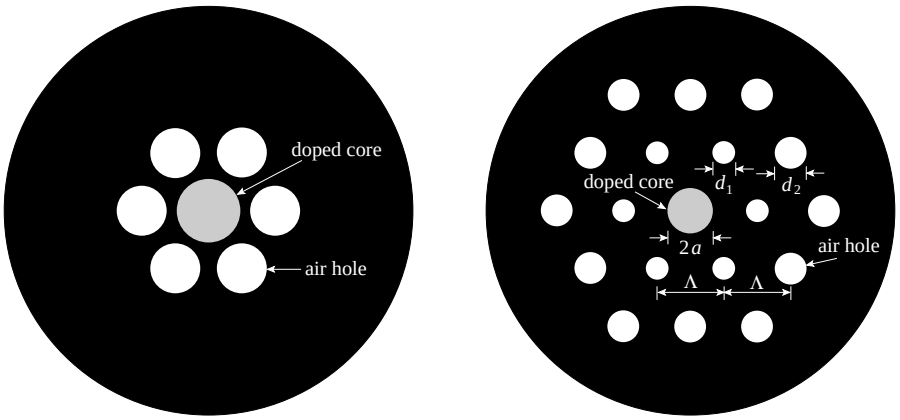

Fig. 1. Schematic representations of HFs with (a) one layer of air-holes and (b) two layers of air-holes.

An optical window between 1.25 μm to 1.625 μm is used in optical transmission systems, so the HF should have a cutoff wavelength lower than 1.25 μm. It is worth to notice that it is difficult to determine an exact cutoff wavelength in hole-assisted HF, because the higher-order mode exists in HF as a leaky mode when the effective refractive index of the higher-order mode becomes lower than the outer cladding (silica) index. In this paper the cutoff wavelength is defined numerically such as the corresponding leakage loss being 22 dB/m. In addition, for HF, the bending loss is higher at longer wavelengths. So, here we consider an operating wavelength of 1.65 μm in order to properly define the allowable bending radius. If the total bending loss for 10 turns is less than 0.5 dB at 1.65 μm, then the radius of each turn is defined as the allowable bending radius. Moreover, in order to succeed in a low-loss splicing between the proposed HF and the standard SMF, the MFD of the HF has to be matched with that of the SMF. To compute the minimum required MFD of the HF, in purpose to have total splice losses L_s less than 0.3 dB at 1.55-μm operating wavelength, we employ the well-known formula [7]:

$$L_s = -20\log_{10}\frac{2w_{SMF}w_{HF}}{w_{SMF}^2 + w_{HF}^2} \tag{1}$$

in decibels, where w_{SMF} and w_{HF} are the MFDs of the SMF and the HF, respectively. Figure 2 shows the MFD dependence of splice loss between the HF and the SMF, where the MFD of the SMF is assumed to be 11.4 μm. We can determine that the minimum value of the MFD of the HF is 8.8 μm. We have investigated the optimum structural parameters of the HF in Fig. 1(b). Here, we develop a full vectorial modal solver based on the finite element method (FEM) with anisotropic perfectly matched layer for the calculations of the cutoff wavelength, the bending loss, and the MFD.

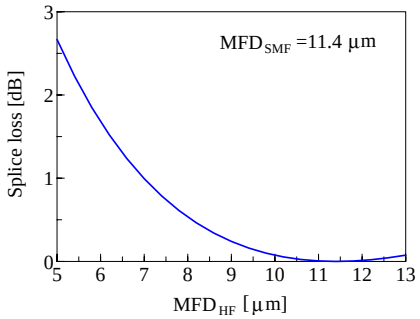

Fig. 2. MFD dependence of splice loss, L_s, between the HF and the SMF, where the MFD of the SMF, w_{SMF}, is assumed to be 11.4 μm.

3. Finite element method for bending loss evaluation

We consider a curved HF as shown in Fig. 3. We assume a circular bend structure, and perfectly matched layer (PML) is used along the radiation direction (+x direction) for suppressing spurious reflection, where R is the curvature radius, d_{PML} is the PML thickness, and x_{PML} is the x coordinate of the PML surface. In the present analysis, we replace the curved HF by a straight fiber with equivalent refractive index as [8]

$$n_{eq}(x, y) = n(x, y)\left(1 + \frac{x}{R}\right), \tag{2}$$

where $n(x, y)$ is the original refractive index profile of the HF. We should notice that the equivalent refractive index $n_{eq}(x, y)$ in the PML region is no longer homogeneous along the x-

direction. Here, we apply the anisotropic PML [9],[10] to this problem. In the anisotropic PML region, the original position vector $\boldsymbol{r} = [x, y, z]^T$ is converted by [9]

$$\tilde{\boldsymbol{r}} = [\tilde{x}, \tilde{y}, \tilde{z}]^T = \left[\int_0^x S(x')dx', y, z \right]^T, \tag{3}$$

where $\tilde{\boldsymbol{r}}$ is the coordinate converted position vector, $S(x)$ is the complex stretching variable [9], and ^{T} denotes a transpose.

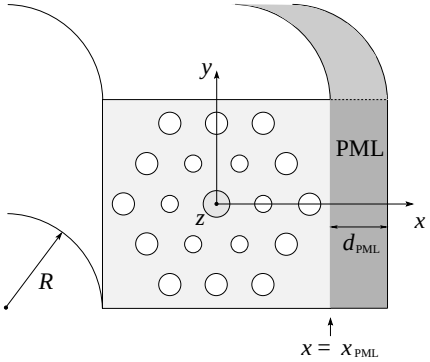

Fig. 3. Curved holey fiber with perfectly patched layer.

Assuming the parabolic profile of the complex stretching variable $S(x)$ as [10]

$$S(x) = \begin{cases} 1 & \text{for } x \le x_{PML} \\ 1 - j\alpha \left(\dfrac{x - x_{PML}}{d_{PML}} \right)^2 & \text{for } x > x_{PML} \end{cases}, \tag{4}$$

the coordinate conversion is expressed as follows:

$$\tilde{x} = \begin{cases} x & \text{for } x \le x_{PML} \\ \left[1 - j\dfrac{\alpha}{3} \left(\dfrac{x - x_{PML}}{d_{PML}} \right)^2 \right] (x - x_{PML}) + x_{PML} & \text{for } x > x_{PML} \end{cases} \tag{5}$$

$$\tilde{y} = y \tag{6}$$

$$\tilde{z} = z, \tag{7}$$

where α is the attenuation parameter in the PML region. Introducing a new electric field vector, $\overline{\overline{\boldsymbol{E}}}$, defined as [9]

$$\overline{\overline{\boldsymbol{E}}} = [S]^{-1} \boldsymbol{E}(\tilde{\boldsymbol{r}}), \tag{8}$$

with

$$[S] = \begin{bmatrix} 1/S(x) & 0 & 0 \\ 0 & 1 & 0 \\ 0 & 0 & 1 \end{bmatrix}, \tag{9}$$

we have the following basic equation for the vector FEM:

$$\nabla\times([S]^{-1}\nabla\times\overline{\overline{\boldsymbol{E}}})-k_0^2 n_{eq}^2(\tilde{\boldsymbol{r}})[S]\overline{\overline{\boldsymbol{E}}}=\boldsymbol{0}\,, \tag{10}$$

where $\boldsymbol{E}(\tilde{\boldsymbol{r}})$ is the coordinate converted electric field vector, k_0 is the free-space wavenumber, and $n_{eq}(\tilde{\boldsymbol{r}})$ is the coordinate converted equivalent refractive index.

In the present formulation curvilinear hybrid edge/nodal elements [11] have been used for accurately modeling curved boundaries. Dividing the fiber cross section into curvilinear hybrid edge/nodal elements and applying the variational finite element procedure, we can obtain the following eigenvalue equation:

$$[K]\{E\}=\beta^2[M]\{E\}\,, \tag{11}$$

where $\{E\}$ is the discretized electric field vector, β is the complex propagation constant, and the finite element matrices $[K]$ and $[M]$ are given in Ref. [10]. The bending loss, L_B, is defined as

$$L_B=8.686\ \mathrm{Im}[\beta] \tag{12}$$

in decibels per meter, where Im stands for the imaginary part.

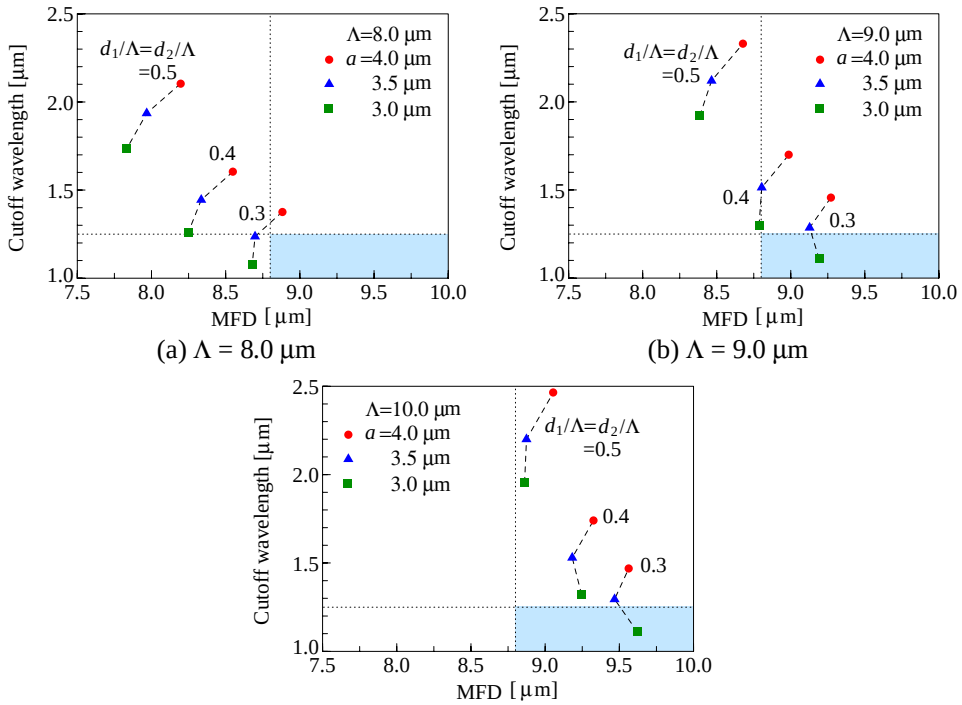

Fig. 4. Relation between the MFD and the cutoff wavelength.

4. The impact of the design parameters to the bending loss and cutoff wavelength characteristics

We consider a hole-assisted fiber structure with two air-hole rings in Fig. 1(b). The centers of all air-holes are arrayed in a regular triangular lattice with the hole pitch Λ. We assume that the Germanium concentration of the core is set up to the level of 0.37 %. This fiber has a step

core similar to the conventional SMFs so that the HF can be spliced to SMFs with low loss even if the holes are filled with silica in fiber splices. As expected, the bending loss as well as the MFD decreases as the value of d_1 increases, while the cutoff wavelength increases. By keeping the parameters d_1 and Λ constant and varying only the value of d_2, we can control the cutoff wavelength and bending loss, without changing the size of the MFD. We perform numerical simulation to obtain the optimum structural parameters, such as the core radius, the hole pitch, and the hole diameters through the vector FEM, where the material dispersion given by a Sellmeier formula is included directly in the calculation.

Figure 4 shows the dependence of the cutoff wavelength on the MFD for various values of parameters Λ, d_1, d_2, and a. We found that the cutoff wavelength is strongly depending on the core radius a, where the MFD of the fundamental mode is evaluated at 1.55-μm wavelength. When the hole pitch Λ is smaller than 8 μm, the MFD takes undesirable small value, resulting in the large splice losses. We can see that, to achieve the desired MFD ($w_{HF} \geq 8.8$ μm) and the desired cutoff wavelength ($\lambda_c \leq 1.25$ μm), we should choose the values of $\Lambda \cong 9.0$ μm, d_1/Λ=0.38, and a=3 μm. The value of $\Lambda \cong 9.0$ μm is the optimum, in the sense that when increases (e.g. Λ=10 μm), the MFD takes undesirable large values, resulting in the large bending losses. Figure 5 shows the impact of the pitch parameter Λ on the allowable bending radius, and we can deduce further optimum values such as d_1/Λ=0.38 and a=3.0 μm, where the bending loss of the fundamental mode is evaluated at 1.65-μm wavelength. Notice that, for the previous parameters, the allowable bending radius is always less than 7 mm. In Fig. 6 we investigate the dependence of the cutoff wavelength on the allowable bending radius, by varying the parameter d_2. We found that by increasing the value of d_2, we can reduce further the allowable bending radius, which results in more compact applications.

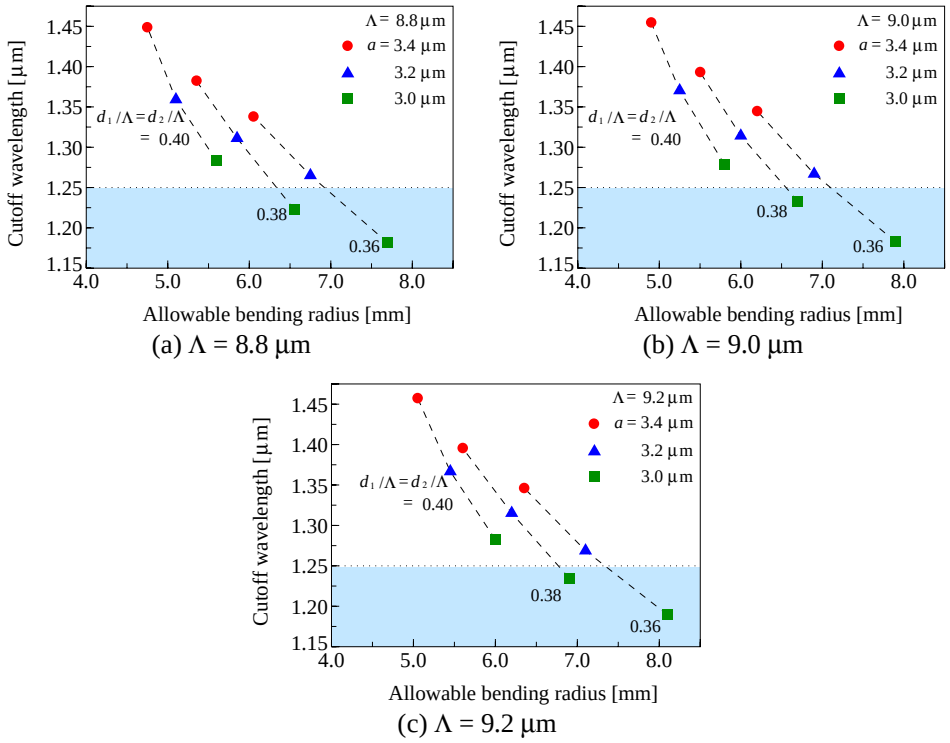

Fig. 5. Dependence of the cutoff wavelength on the allowable bending radius.

Finally, for example, we consider a HF with a=3.0 μm, Λ=9.0 μm, d_1/Λ=0.38, and d_2/Λ=0.40. The MFD is 8.8 μm at 1.55-μm wavelength. The allowable bending radius and the cutoff wavelength for this HF are 5.9 mm and 1.28 μm, respectively. In Fig. 7 we plot the optical field distribution in the curved HF, where the operating wavelength is 1.55 μm and the bending radius is 6.0 mm. As we can see, there is a strong confinement of the light in the core and the radiation into the cladding region is minimized, showing the usefulness of the proposed hole-assisted HF and design procedure.

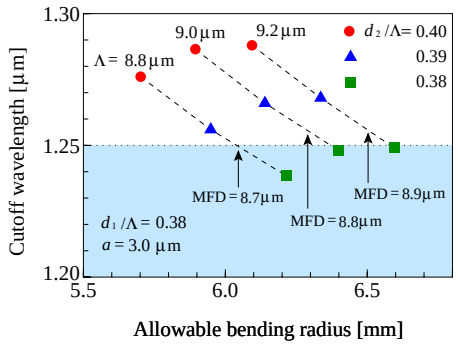

Fig. 6. Dependence of the cutoff wavelength and the allowable bending radius on air-hole diameter of the second ring.

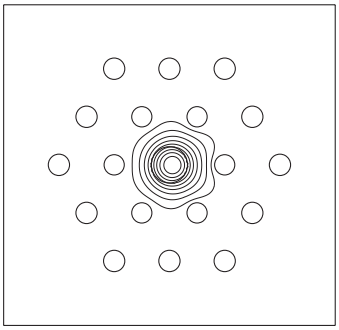

Fig. 7. Optical field distribution in curved HF with bending radius of 6 mm at 1.55-μm wavelength, where a=3.0 μm, Λ=9.0 μm, d_1/Λ=0.38, and d_2/Λ=0.40.

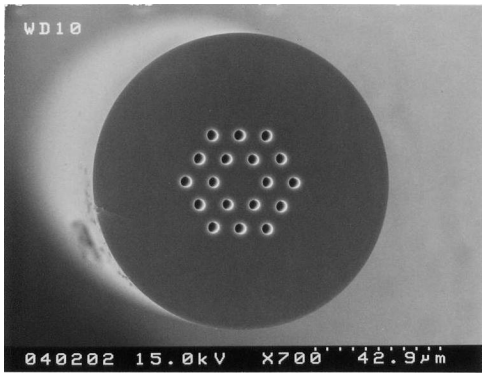

Fig. 8. Cross sectional view of fabricated HF.

Table 1. Characteristics of the fabricated HF at 1.55 μm.

Attenuation [dB/km]		2.3
Mode field diameter [μm]		9.3
Fiber cutoff wavelength [μm]		1.1
Dispersion [ps/(km·nm)]		21.8
Bending loss [dB/turn]	Bending diameter 10 mm	0.011
	Bending diameter 20 mm	0.002

5. Experimental results and discussions

Based on the above design, we have fabricated the bending-insensitive HF shown in Fig. 8, where the core radius a=2.95 μm, the hole pitch Λ=8.98 μm, and the hole diameters are d_1=3.51 μm (d_1/Λ=0.39) and d_2=3.71 μm (d_2/Λ=0.41), respectively. The structural parameters of the fabricated fiber are almost the same as those of the designed fiber. The characteristics of the fiber are summarized in Table 1. Even though this fiber has relatively high transmission loss of 2.3 dB/km at 1.55-μm wavelength, this attenuation can be reduced by careful optimization of the fabrication process. The chromatic dispersion is 21.8 ps/(km·nm) at 1.55 μm. We measured the cutoff wavelength of the fiber using multimode excitation method recommended by ITU-T G.650 with a fiber of 2 m in length and bending radius of 140 mm. The cutoff wavelength of the higher-order mode is 1.1 μm. Figure 9 shows the numerically evaluated wavelength dependence of the effective indices of the fundamental and higher-order modes of the fabricated HF, where the pure silica index is shown as a dotted curve. The effective index of the fundamental mode is higher than the pure silica index, on the other hand, the effective index of the higher-order mode becomes equal to the silica index at ~0.92-μm wavelength. It is noteworthy that the measured cutoff wavelength is longer than the wavelength of intersection between the effective index of the higher-order mode and the pure silica index in Fig. 9, because the higher-order mode exists in HF as a leaky mode when the effective index of the higher-order mode becomes lower than the silica index. Figure 10 shows the wavelength dependence of the leakage loss of the higher-order mode for this fiber. The leakage loss becomes 13 dB/m at 1.25 μm. Figure 11 shows the optical field distributions of the fundamental and higher-order modes at 0.92-μm wavelength, where the contours are spaced by 3 dB. As we can see, the fundamental mode is strongly confined to the core region, while the higher-order mode penetrates more deeply into the cladding region.

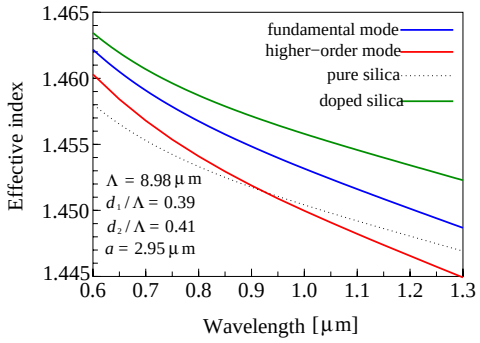

Fig. 9. Wavelength dependence of effective indices of the fundamental and higher-order modes.

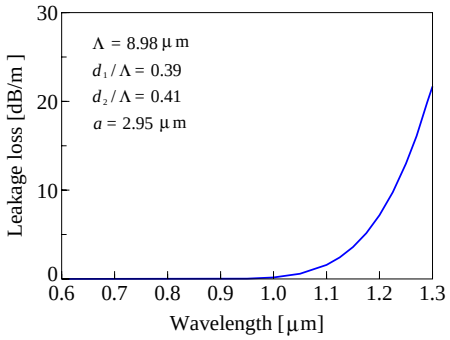

Fig. 10. Dependence of leakage loss of the higher-order mode on the operating wavelength.

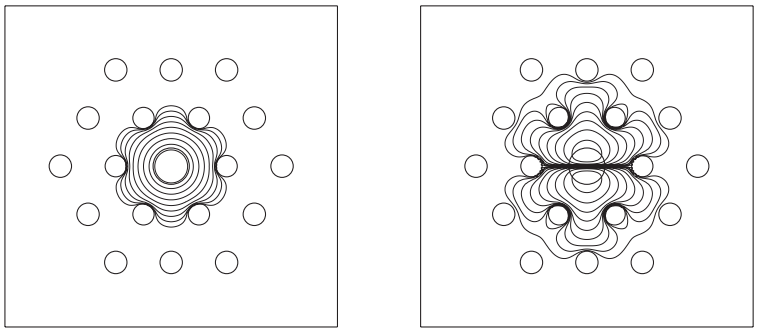

Fig. 11. Optical field distributions of (a) the fundamental and (b) higher-order modes at 0.92-μm wavelength with a=2.95 μm, Λ=8.98 μm, d_1/Λ=0.39, and d_2/Λ=0.41.

Figure 12 shows the experimental and numerical bending loss properties of the HF as a function of bending radius at 1.55-μm wavelength. For comparison, the experimental bending loss of standard SMF is also plotted. We can see that the bending loss of the HF is much lower than that of the SMF especially for small bending radius and 0.011 dB/turn for bending radius of 5 mm at 1.55 μm. The calculated results are in good agreement with the experimental ones, showing the validity of our numerical design procedure. The MFD of the HF is 9.3 μm at 1.55-μm wavelength. Although this MFD is smaller than that of a typical SMF, it would be possible to splice the SMF with low loss because the HF with collapsed air holes has almost same MFD with that of the SMF. Figure 13 shows the histogram of the splicing loss for HF and SMF at 1.55 μm using a commercial arc fusion splicer. We measured the splice loss to be 0.08 dB per fusion-splice on average, which would be allowable in practical use. It is worth noting that Hasegawa *et al.* [5] have formed a taper region for gradual MFD transition to splice a HF with an SMF, on the other hand, the proposed HF can be spliced to an SMF by only arc fusion splicing with low loss. If we keep the hole diameter d_1 in the inner layer and the hole pitch Λ constant and increase the hole diameter d_2 in the outer layer, we can further reduce the bending loss without changing the MFD.

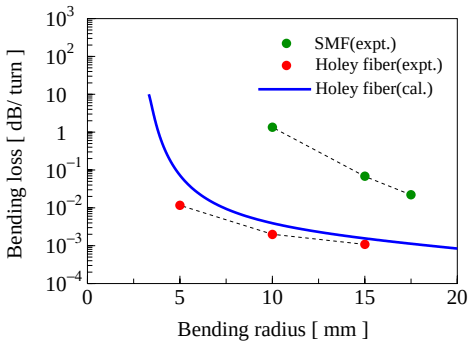

Fig. 12. Bending loss property as a function of bending radius at 1.55 μm.

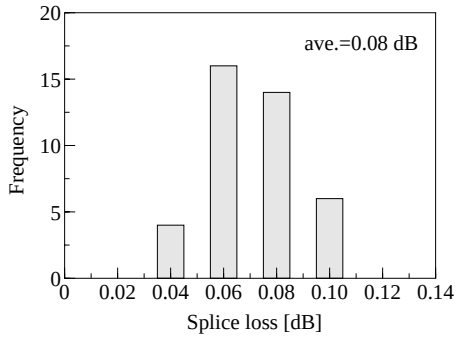

Fig. 13. Splice loss histogram for fusion splicing between HF and SMF at 1.55 μm.

6. Conclusions

We have proposed and demonstrated a novel type of bending-insensitive single-mode hole-assisted holey fibers for optical interconnection applications. The holey fibers with a doped core and two layers of holes with different air-hole diameters have been designed. It has been shown through numerical and experimental results that it is possible to design a holey fiber with a MFD of 9.3 μm at 1.55-μm wavelength, a small bending loss of 0.011 dB/turn at 1.55 μm for bending radius of 5 mm, and a cutoff wavelength below 1.1 μm, by appropriately choosing the core radius, the hole pitch, and the air-hole diameters.